

High-spectral-efficiency transmission of PDM 256-QAM with Parallel Probabilistic Shaping at Record Rate-Reach Trade-offs

S. Chandrasekhar, B. Li, J. Cho, X. Chen, E. C. Burrows, G. Raybon, and P. J. Winzer

Nokia Bell Labs, 791 Holmdel Road, Holmdel, NJ 07733 USA.
 chandra.sethumadhavan@nokia-bell-labs.com

Abstract We demonstrate the transmission of near-optimal low-complexity probabilistically shaped PDM 256-QAM over multiple low-loss all-Raman amplified 50-km large effective area fiber spans, with spectral efficiencies from 14.1 b/s/Hz to 8.9 b/s/Hz at reaches from 500 km to 4000 km.

Introduction

Coherent optical communications has adopted a host of tools from classical communications engineering to closely approach the Shannon limit, including polarization-division multiplexing (PDM), higher-order quadrature amplitude modulation (QAM), multi-dimensional symbol constellations, pulse shaping, forward error correction (FEC), and sophisticated linear and non-linear digital signal processing (DSP) techniques. The latest concept to attract significant attention in fiber-optic communications has been probabilistic shaping^{1,2} (PS), not only for its ability to extract some extra shaping gain but also to facilitate flexible transponders that can dynamically adapt their information rate (and with it the system’s spectral efficiency, SE) to the desired system reach³.

In this paper, we demonstrate a widely flexible transponder that uses a novel, low-complexity PS scheme based on prefix codes to achieve close-to-optimum shaping performance while requiring only simple look-up table searches and allowing for highly parallelized application specific integrated circuit (ASIC) implementation. Using this scheme, we demonstrate dense wavelength-division multiplexed (WDM) transmission using full FEC decoding. With five 16-GBaud PS PDM 256-QAM channels on a 16.2-GHz grid, we achieve a flexible rate-reach trade-off at record performance over $N \times 50$ -km spans in a 5-span recirculating loop made of all-Raman amplified low loss, large effective area fiber. Our results are shown in Figure 1 together with other record transmission experiments, including regular WDM experiments (white) and spectrally narrowly confined single-channel experiments (gray); for the latter, the data points represent upper bounds to a potentially achievable SE. Two previous experiments (red¹ and blue⁴) used PS to trade off rate and reach as we do in this paper, but Ref. 1 used only a *single WDM channel*; Ref. 4 used five 10-GBaud signals, but on a 25-GHz grid, which leads to a significant reduction in SE compared to their reported per-channel achievable

information rates (AIR_{Ch}). Hence, as an upper bound to the potentially achievable SE performance of Refs. 1 and 4, we show in Fig. 1 their AIR_{WDM} , their (dual-polarization) AIR_{Ch} scaled back by their spectral excess bandwidths, $AIR_{WDM} = AIR_{Ch} / (1+r)$, where r is their root raised cosine (RRC) roll-off factor (diamonds). Our results (yellow) clearly achieve record AIR_{WDM} over a wide range of rate/reach combinations, with AIR_{WDM} ranging from 14.1 b/s/Hz at 500 km to 8.9 b/s/Hz at 4000 km. Similarly, we scale back the actually decoded results of Refs. 1 and 4 (circles), and for our system report 12.6, 11.4, and 10.1 b/s/Hz at 500, 1000, and 2000 km. This record performance fills the wide gap between Ref. 5, which demonstrated 14 b/s/Hz over 720 km, albeit at only 2.5 GBaud and in self-homodyne operation, and Ref. 6, which got 8.3 b/s/Hz over 6375 km.

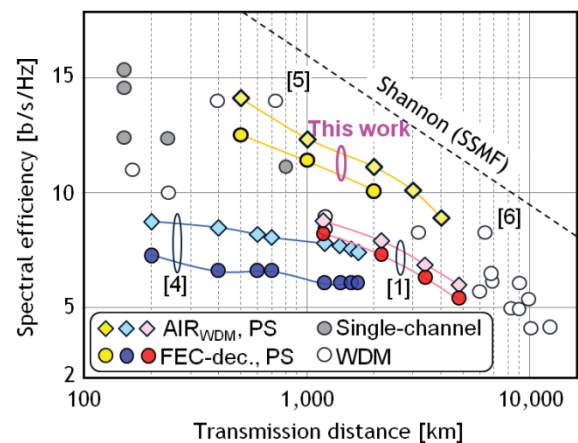


Fig. 1: Experimentally achieved SE-reach trade-offs.

Experimental Setup and DSP

The experimental setup is shown in Figure 2. A 1-kHz linewidth external cavity laser (ECL1) at 193.397 THz is used to generate a total of 5 carriers with 16.2-GHz spacing. The laser power is split in two, each portion amplified and followed by Mach-Zehnder modulators (MZMs) to generate three and two 32.4-GHz spaced carriers, respectively. The MZMs are sinusoidally driven, one at 32.4 GHz (odd carriers), and one at 16.2 GHz (even carriers). Even and odd car-

riers are modulated independently by LiNbO₃ PDM in-phase/quadrature (I/Q) modulators, driven by two 4-channel digital-to-analog converters (DACs) at 88 GSa/s to produce 16-GBaud RRC PDM 256-QAM (0.01 roll-off) from 16 independent pseudo-random bit patterns of length 2¹⁴. The modulated signals are amplified and passively combined. The WDM signal enters a recirculating loop consisting of five 50-km spans of Corning® Vascade® EX2000 fiber with an average loss, dispersion, and effective area at 1550 nm of 0.16 dB/km, 20.1 ps/nm/km, and 112 μm². The span loss is fully compensated by backward Raman amplification. An EDFA compensates for loop related losses (loop switches and ASE filter). At the receiver, a second free-running ECL of the same type as ECL1 is used to generate 5 carriers at 16.2-GHz spacing by a 3rd MZM, driven at 16.2-GHz. A wavelength selective switch (WSS) selects one of the 5 carriers to serve as optical local oscillator (OLO) for intradyne detection. A 2nd WSS is used to scan the 5 WDM channels. A PDM 90-degree hybrid with balanced detection and 4 analog-to-digital converters (ADCs) at 80 GSa/s, embedded in a real-time oscilloscope, acts as coherent front-end. The scope bandwidth is set to 10 GHz.

Off-line DSP is performed on multiple captures of 2x10⁶ samples each. Resampling to 2 samples/symbol, chromatic dispersion compensation and polarization demultiplexing using pilot-assisted pre-convergence with least-mean square (LMS) equalization is followed by blind LMS equalization and blind carrier phase recovery. Only the blindly recovered data are used for subsequent performance evaluation.

Probabilistic Shaping and FEC

Probabilistic shaping of the 256-QAM symbols is realized by two-dimensional 16-level amplitude shaping, independently for the I and Q components of the QAM signal. Variable-length prefix codes are used for PS. A novel algorithm, with which a fixed-length input bit block always produces a fixed-length output amplitude block, solves the variable-length problems of prefix

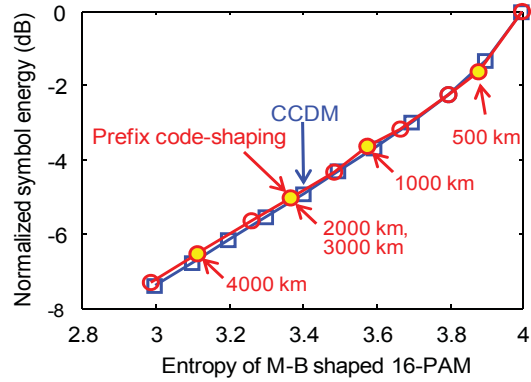


Fig. 3: Normalized average energy of the PS symbols.

codes, such as⁷ buffer overflow, boundless error propagation, and frame resynchronization. A 64-entry codebook is constructed for a desired probabilistic distribution, which can be implemented by a small look-up table (< 256 bytes), avoiding the computationally demanding arithmetic coding used in constant composition distribution matching⁸ (CCDM). Starting from a target entropy value, we choose a codebook to render equiprobable information bits into Maxwell-Boltzmann (M-B) distributed 16-level symbols. The average energy of the shaped QAM symbols is shown in Fig. 3, normalized to the average energy of uniformly distributed square-QAM symbols. Our approach (circles) comes close to the near-optimum results achieved by CCDM (squares). The 4 values used in our transmission experiment are indicated as well.

To quantify system performance, we assume bit-interleaved coded modulation (BICM) with systematic FEC codes such that the shaped symbol distribution is preserved under FEC coding⁹. The generalized mutual information for bit-metric decoding in two polarizations (GMI_{BMD}), which is the (dual-polarization) AIR under our binary FEC decoding assumption, is estimated using an additive white Gaussian noise auxiliary channel whose noise variance is obtained from the received constellations⁹. We then scale back AIR_{Ch} by the actual WDM channel spacing, AIR_{WDM} = AIR_{Ch} × 16 / 16.2 as an even more

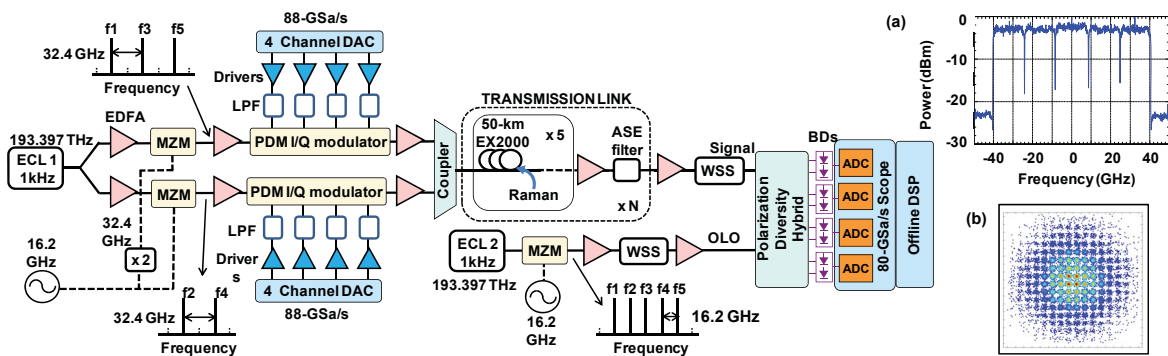


Fig. 2: Schematic of the experimental setup. Insets: (a) optical spectrum of the 5-channel WDM system (back-to-back); (b) recovered probabilistically shaped constellation for one polarization for channel 3 (back-to-back).

realistic metric than only scaling back by r . This yields an upper bound to the WDM SE, achievable for perfect decoding with a capacity-achieving soft-decision (SD) FEC. *In addition*, we also perform *actual SD-FEC decoding* to evaluate an SE that can be truly achieved with existing non-ideal codes. To this end, we use min-sum decoding of a 20% and a 25% overhead (OH) spatially-coupled low-density parity-check (SC-LDPC) code¹⁰, whose known error floor at a post-FEC BER of $\sim 10^{-11}$ is removed by a 0.8% overhead outer HD-FEC, a BCH (8191, 8126, 5), with a correction threshold of 1.1×10^{-6} . The reported decoded SEs take into account both FEC OHs and the WDM channel spacing. Figure 4 shows the decoding performance of the 25% OH SD-FEC at 2000 km, revealing an extremely sharp decoding edge.

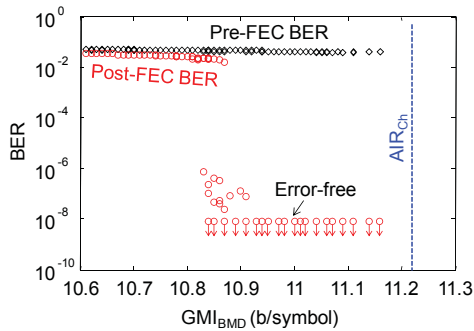


Fig. 4: Performance of the 25%-OH SC-LDPC code with probabilistic shaping at 2000 km (GMI in both polarizations).

Experimental Results

Measurements are first made using a uniform square-QAM constellation to determine an optimum per-span signal launch power between -8 and -9 dBm per channel; this range is used in all measurements. Figure 5 shows the AIR_{Ch} and the pre-FEC Q-factor for all 5 WDM channels after 2000-km transmission with PS, showing uniform performance to within ± 0.1 dB. All channels are verified to be correctable to below the HD-FEC threshold by the SD-FEC described above.

Figure 6 compares transmission performance using uniform and PS constellations from 500 to 4000 km. The system is highly flexible in its rate-reach trade-off, allowing a variation of AIR_{WDM} as an upper bound to the actual SE from 14.1 b/s/Hz at 500 km to 8.9 b/s/Hz at 4000 km. The

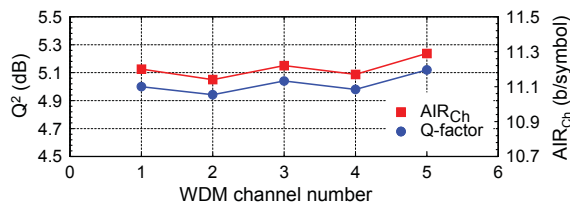


Fig. 5: Received Q-factor and AIR_{Ch} for each of the five channels in the WDM system at 2000 km with PS.

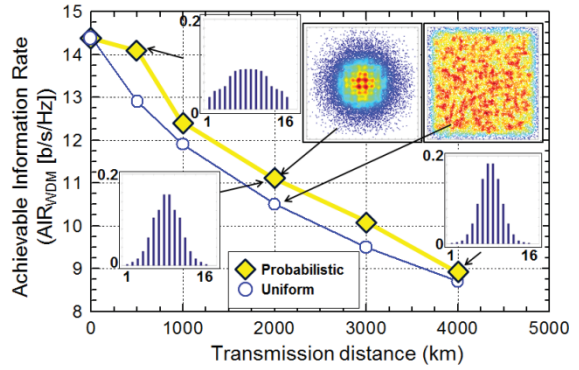


Fig. 6: AIR_{WDM} vs. transmission distance. Inset: Recovered x-pol. constellations at 2000 km, along with the PS symbol distributions used at three distances.

gain from shaping is about 0.6 b/s/Hz at constant reach. In terms of reach at constant SE, PS provides 90% to 10% of gain.

From the AIR_{Ch} and the shaping parameter we extract the need for FEC OHs between 8.2% and 28.4%. As we only had two actual SD-FEC codes with known complexity and performance available¹⁰, we used these 20% and 25% OH codes to verify decoding performance at 500 km (20% OH), 1000 km (20% OH), and 2000 km (25% OH). The SEs shown by yellow circle markers in Fig. 1 are actually decoded values, taking into account SD- and HD-FEC OHs as well as the WDM channel spacing.

Note that although we only demonstrate 5 specific rate-reach trade-offs in Figs. 1 and 6, a much larger number could be constructed with our PS algorithm for an almost continuous rate-reach adaptation, such that any point on or near the lines connecting the demonstrated results could be reached.

Conclusions

We have demonstrated widely flexible transmission using probabilistically shaped PDM 256-QAM in a dense WDM system with actual FEC decoding. We have achieved a wide range of transmission distances from 500 to 4000 km at record SE performance.

The authors thank Corning Inc. for the loan of the Vascade EX2000 fiber.

References

- [1] F. Buchali et al., JLT **34**, 1599 (2016).
- [2] W. Idler et al., Proc. ECOC, M1.D.2 (2016).
- [3] X. Zhou et al., IEEE ComSoc. Mag. **51**, 41 (2013).
- [4] M. P. Yankov et al., arXiv:1603.07327v1 (2016).
- [5] T. Omiya et al., Opt. Ex. **21**, 2632 (2013).
- [6] S. Zhang et al., Proc. OFC-PD, Th5C.2 (2016).
- [7] P. Schulte et al., IEEE Trans. IT **62**, 430 (2016).
- [8] G. Böcherer et al., Proc. ISIT, 431 (2014).
- [9] A. Alvarado et al., JLT **33**, 4338 (2015).
- [10] J. Cho et al., Proc. ICC, 6028 (2015).